



Communication

Ultrasonic Auxiliary Ozone Oxidation-Extraction Desulfurization: A Highly Efficient and Stable Process for Ultra-Deep Desulfurization

Rui Wang ^{1,*} , Kaiqing Zhang ¹ and Ivan V. Kozhevnikov ² ¹ School of Environmental Science & Engineering, Shandong University, Qingdao 266237, China² Department of Chemistry, The University of Liverpool, Liverpool L69 7ZD, UK

* Correspondence: wangrui@sdu.edu.cn

Abstract: For ultra-deep desulfurization of diesel fuel, this study applied the ultrasound-assisted catalytic ozonation process to the dibenzothiophene (DBT) removal process with four Keggin-type heteropolyacids (HPA) as catalysts and acetonitrile as extractant. Through experimental evaluations, $H_3PMO_{12}O_{40}$ was found to be the most effective catalyst for the oxidative removal of DBT. Under favorable operating conditions with a temperature of 0 °C, $H_3PMO_{12}O_{40}$ dosage of 2.5 wt.% of *n*-octane, and ultrasonic irradiation, DBT can be effectively removed from simulated diesel. Moreover, the reused catalyst exhibited good catalytic activity in recovery experiments. This desulfurization process has high potential for ultra-deep desulfurization of diesel.

Keywords: ultra-deep desulfurization; heteropoly compound; dibenzothiophene



Citation: Wang, R.; Zhang, K.; Kozhevnikov, I.V. Ultrasonic Auxiliary Ozone Oxidation-Extraction Desulfurization: A Highly Efficient and Stable Process for Ultra-Deep Desulfurization. *Molecules* **2022**, *27*, 7889. <https://doi.org/10.3390/molecules27227889>

Academic Editor: Giancarlo Cravotto

Received: 3 September 2022

Accepted: 7 November 2022

Published: 15 November 2022

Publisher's Note: MDPI stays neutral with regard to jurisdictional claims in published maps and institutional affiliations.



Copyright: © 2022 by the authors. Licensee MDPI, Basel, Switzerland. This article is an open access article distributed under the terms and conditions of the Creative Commons Attribution (CC BY) license (<https://creativecommons.org/licenses/by/4.0/>).

1. Introduction

Ultra-deep desulfurization from transportation fuels has become an increasingly important subject worldwide, due to urgent environmental problems and increasingly stringent regulations. Conventional catalytic hydrodesulfurization (HDS) is highly efficient in removing aliphatic and acyclic sulfur compounds, but is limited to reducing refractory sulfur-containing compounds such as dibenzothiophene (DBT) and its derivatives to ultra-low levels [1]. Therefore, it is urgent to develop alternative non-HDS methods to achieve clean fuels with extremely low sulfur concentrations.

One of the most promising alternative methods is oxidative desulfurization (ODS) combined with the extraction process. Compared with conventional HDS, refractory sulfur compounds can be removed under mild conditions in ODS [2]. Aqueous H_2O_2 is the commonly used oxidant [3]. However, the catalyzed decomposition of hydrogen peroxide may compete with sulfur-containing compound oxidation in the catalytic oxidative desulfurization process, which would cause the consumption of a huge amount of hydrogen peroxide [4].

Ozone, due to its high oxidation potential (2.07 V in acid solution) [5] and environmentally friendly nature, is widely applied in water treatment as well as in other fields [6,7]. Although ozone is a green catalyst with strong oxidizing properties, this catalyst is unstable [8]. Ozone is poorly soluble in oil products. Its oxidation effect is not satisfactory when the ozone concentration is too low [9]. Too high a level of ozone concentration is harmful to the environment and causes a drop in octane number affecting oil quality. Therefore, the proper ozone concentration should be selected in the ODS system. Heteropoly compound, an increasingly important class of environmentally friendly catalysts for various organic reactions [10], has recently attracted considerable attention. Shatalo et al. [11,12] found that molybdo-vanado-phosphate heteropolyanion catalyzing pulp ozonation in acetone/water solution was a particularly effective and selective environmentally benign bleaching approach. Therefore, it is possible that catalytic ozonation by Keggin heteropolyacids may show potential benefits in desulfurization.

Recent studies of catalytic desulfurization with Keggin heteropolyacids have focused on the preparation of loaded catalysts to improve catalytic efficiency. For example, Craven et al. [13] prepared POM/RPN-SiO₂ catalysts by immobilizing POM (PMo, PW, and SiW) on RPN-SiO₂ carriers using the corresponding heteropolyacids as precursors. The catalytic efficiencies of PMo, PW, and SiW in DBT oxidation were 100%, 70%, and 55%, respectively, after 3 h of catalytic reaction using 30% H₂O₂ as the oxidant. Rafiee et al. [14] incorporated three heteropolyacids, including H₃PMo₁₂O₄₀ (PMo), H₃PW₁₂O₄₀ (PW), and H₄SiW₁₂O₄₀ (SiW), into HKUST-1 used for the catalytic oxidation of sulfides. The experimental results showed that the catalytic efficiency of POMS for sulfide decreases in the order of PMo > PW > SiW. Mesoporous LaVO₄ for deep desulfurization was prepared by the hydrothermal method by Hussain et al. [15]. A photocatalytic approach was taken to remove organic sulfur compounds from diesel and this catalyst had good desulfurization efficiency under mild reaction conditions. Li et al. [16] selected MIL-101 (Al) and MIL-101 (Fe) for the immobilization of the active ingredient H₃PMo₆W₆O₄₀, and such catalysts had extremely high catalytic efficiency in the oxidation of DBT. Since then, Li et al. [17] have synthesized a POM-modified catalyst (POM-MIL-101F@Fibercloth), which has an excellent degradation rate for DBT under the condition of ethanol as solvent. However, there are few studies on catalytic ozone desulfurization and ultrasound-assisted desulfurization.

Based on the previous study of some metal salts of Keggin-type heteropolyacids as oxidative desulfurization catalysts by our group [18], four different types of Keggin-type heteropolyacids (HPA) were used as catalysts, and acetonitrile was used as an extractant for DBT removal. Main factors affecting the desulfurization process, including temperature, catalyst dosage, initial sulfur content, and ultrasonic irradiation, were investigated, and DBT was found to be removed effectively by this system under optimized conditions. Moreover, the recovered catalyst exhibited good catalytic activity.

2. Experimental Section

2.1. Materials

All reagents and solvents were available commercially and used without further purification, unless indicated otherwise. DBT (C₁₂H₈S, 99%) was purchased from Sigma-Aldrich. BT (C₈H₆S, 98%) and 4,6-DMDBT (C₁₄H₁₂S, 97%) were purchased from J & K Chemical Ltd. (Beijing, China). AR-grade phosphomolybdic acid (H₃PMo₁₂O₄₀·xH₂O), phosphotungstic acid (H₃PW₁₂O₄₀·xH₂O), and silicotungstic acid (H₄SiW₁₂O₄₀·xH₂O) were purchased from the National Drug and Chemical Group Co., Ltd. (Tianjin, China). The solution of DBT in *n*-octane was used as simulated diesel, in which the sulfur content was set by fixing the dosage of DBT. Ozone was produced from pure oxygen using an ozone generator.

2.2. Catalyst Preparation

H₃PW₁₂O₄₀·xH₂O, H₃PMo₁₂O₄₀·xH₂O and H₄SiW₁₂O₄₀·xH₂O were pretreated according to literature [19,20] to obtain H₃PW₁₂O₄₀·6H₂O, H₃PMo₁₂O₄₀·13H₂O, and H₄SiW₁₂O₄₀·6H₂O.

H₄GeW₁₂O₄₀ was prepared according to the method given by Wu [21]. Germanium powder (2.625 g) was suspended in 15 mL of NaOH solution (6.25 mol/L). An aqueous H₂O₂ solution (~10 mol/L) was dropped slowly into the above mixture, stirring until complete metal dissolution. The obtained solution was moved into a water bath at 80 °C to decompose the hyperoxide until no further O₂ evolution, then diluted into 100 mL, thus a germanate stock solution was obtained.

125 mL of the aqueous solution of Na₂WO₄ (1.25 mol/L) was mixed with 35 mL of germanate stock solution and the mixture was warmed up to 80 °C. The pH of the mixture solution was adjusted to 0.5 using concentrated aqueous HNO₃. After the reaction proceeded for 1 h at 80 °C, the solution was cooled to room temperature. The cooled solution was extracted with ether in a sulfuric acid medium. The extractant was dissolved

with a little water and then the ether was removed by flowing dry air. The remaining solution was kept in a vacuum desiccator until crystallization. The yield was about 30 g.

2.3. Catalyst Characterization

The properties of $H_4GeW_{12}O_{40}$ prepared were characterized by FT-IR, TG-DSC, XPS, XRD and BET. Fourier transform infrared (FT-IR) spectra were recorded on a 5DXC IR spectrometer in the wave number interval between 4000 and 400 cm^{-1} with a 2 cm^{-1} resolution, and samples were measured with KBr pellets. TG-DSC was performed on an SDT Q600 Universal V4.1D TA instrument operating under a nitrogen flow of 20 mL/min, at a $10\text{ }^\circ\text{C}/\text{min}$ heating rate up to $700\text{ }^\circ\text{C}$ and using 25–50 mg sample. X-ray diffraction (XRD) patterns were collected by a PAN alytical X-pert 3 instrument using a $\text{CuK}\alpha$ -ray source ($\lambda = 0.154\text{ nm}$, $40\text{ mA} \times 40\text{ kV}$) with a scanning speed of 15° min^{-1} . The elemental composition was tested by an ESCALAB 250Xi X-ray energy spectrometer. The specific surface area and porosity of the materials were measured by Micromeritics ASAP 2460.

2.4. Experimental Method

A schematic diagram of the ozonation system is shown in Figure 1. A three-necked 250 mL round-bottomed flask was used as an ozonation reactor for the desulfurization experiments. The middle neck connected with a gas disperser through which ozone was introduced into the reaction solution at a constant rate. One of the two side necks connected with a water-cooled reflux condenser to prevent reaction solution loss and to serve as a gas outlet, and the residual ozone in the outlet gas was adsorbed by KI solution. The other was closed with a glass stopper. After 60 mL of simulated diesel and 60 mL of acetonitrile were added to the flask, the catalyst was added to the above mixture, and then ozone was bubbled up into the mixture. Sonication was performed with a KQ-100 KDB ultrasonic generator (100 W, 20 kHz, Kunshan Ultrasonic Instrument Co., Ltd., Suzhou, China). The flask was immersed into the ultrasonic bath, inside which a temperature control system was placed to keep a certain temperature, and a low temperature was achieved by adding ice to the ultrasonic bath. During the reactions, the upper *n*-octane phase of the reaction mixture was periodically withdrawn and determined for sulfur content using a Model WK-2E microcoulometric integrated analyzer (Jiangsu Jiang Fen Electroanalytical Instrument Co., Ltd., Taizhou, China).

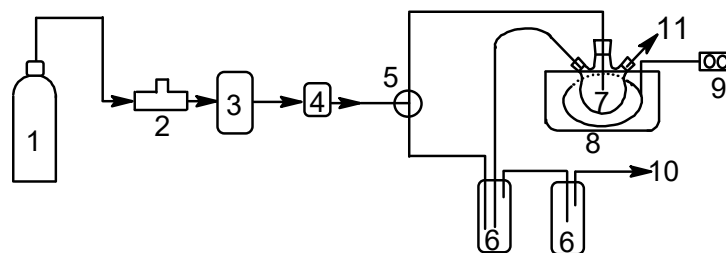


Figure 1. Diagram of the experimental setup. (1) oxygen cylinder; (2) mass flow controller; (3) ozone generator; (4) ozone monitor; (5) three-way valve; (6) KI traps (7) ozone reactor; (8) ultrasonic generator; (9) temperature control system; (10) gas outlet; (11) sampling.

3. Discussion

3.1. Characterizations of the Catalysts

Characteristic vibration bands of Keggin structure appear in the region of 700 cm^{-1} to 1100 cm^{-1} [22]. As shown in Figure 2a, the IR spectrum of $H_4GeW_{12}O_{40}$ shows strong vibration bands at 983, 892, 817, and 767 cm^{-1} , which correspond respectively to the asymmetric vibrations W-Od (terminal O bonded to W), W-Ob (edge-sharing O connecting W), Ge-Oa (internal O atom connecting Ge and W), and W-Oc (corner-sharing O connecting W_3O_{13} units) [23]. Hence, the desired 12-tungstogermanic acid with Keggin structure can be confirmed according to the presence of these adsorption peaks.

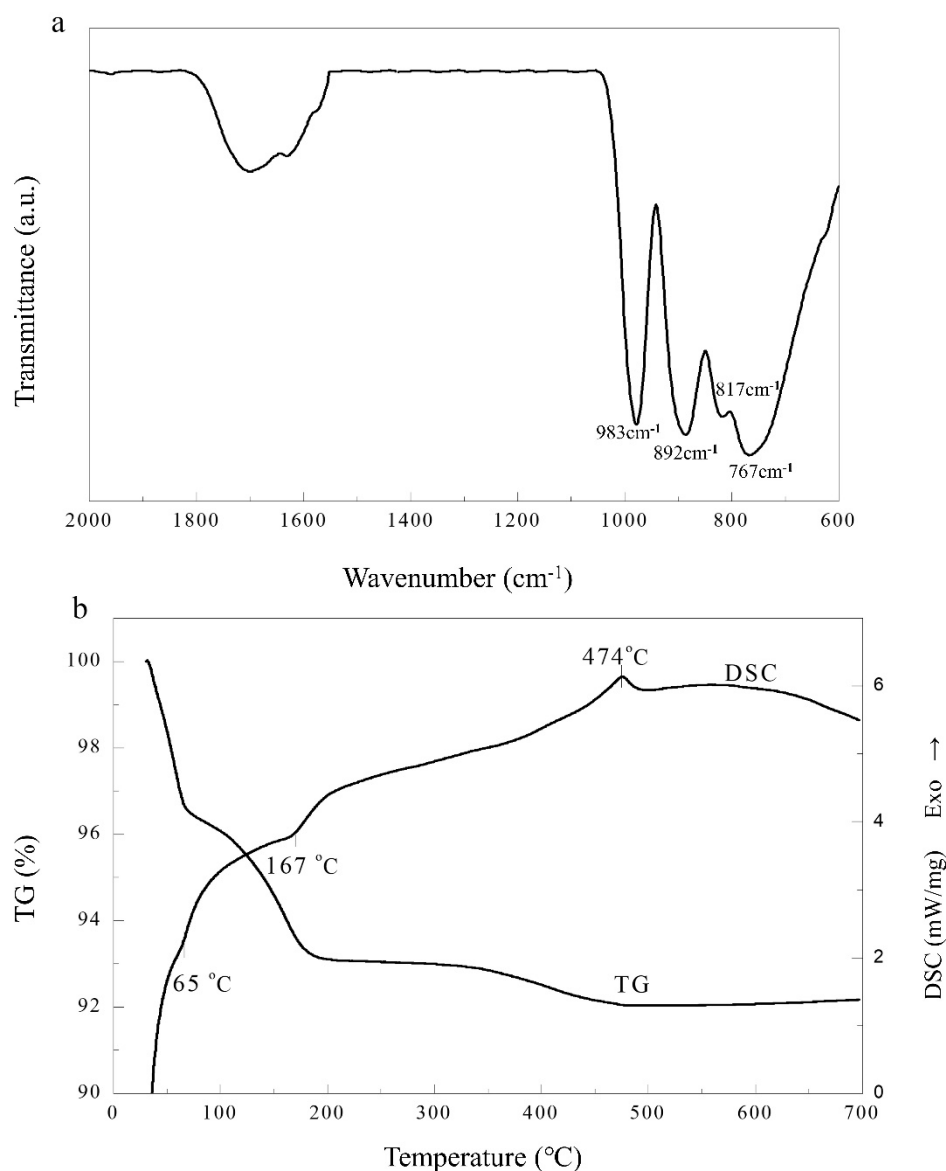


Figure 2. (a) FT-IR spectra of the $\text{H}_4\text{GeW}_{12}\text{O}_{40}$. (b) TG–DSC curves of $\text{H}_4\text{GeW}_{12}\text{O}_{40}$.

The thermal behavior of the hydrated $\text{H}_4\text{GeW}_{12}\text{O}_{40}$ was investigated by TG-DSC, and the results are shown in Figure 2b. There were three steps of weight loss in the TG curve. Before 70 °C and between 70–202 °C, the mass losses were both 3.45%, which demonstrated that six molecules of zeolite water and six molecules of protonized water were lost [19,24]. The DSC curve showed two corresponding endothermic peaks at 65 and 167 °C due to the release of zeolite water and protonized water, respectively. Above 202 °C, the slow weight loss of 1.06% in the TG curve can be attributed to the departure of two molecules of structural water, and an exothermic peak centered at 474 °C in the DSC curve was due to the decomposition of $\text{H}_4\text{GeW}_{12}\text{O}_{40}$, consistent with the result studied by Wang et al. [20]. Thus, the formula of tungstogermanic heteropoly acids synthesized in this paper was $\text{H}_4\text{GeW}_{12}\text{O}_{40}\cdot 12\text{H}_2\text{O}$.

The XRD pattern of $\text{H}_4\text{GeW}_{12}\text{O}_{40}$ is shown in Figure 3. The curves showed strong characteristic diffraction peaks in the ranges of 15–23°, 26–33° and 36–39°, indicating that $\text{H}_4\text{GeW}_{12}\text{O}_{40}$ has a Keggin-type structure, which is consistent with reports in the literature [25]. This indicates the successful synthesis of $\text{H}_4\text{GeW}_{12}\text{O}_{40}$.

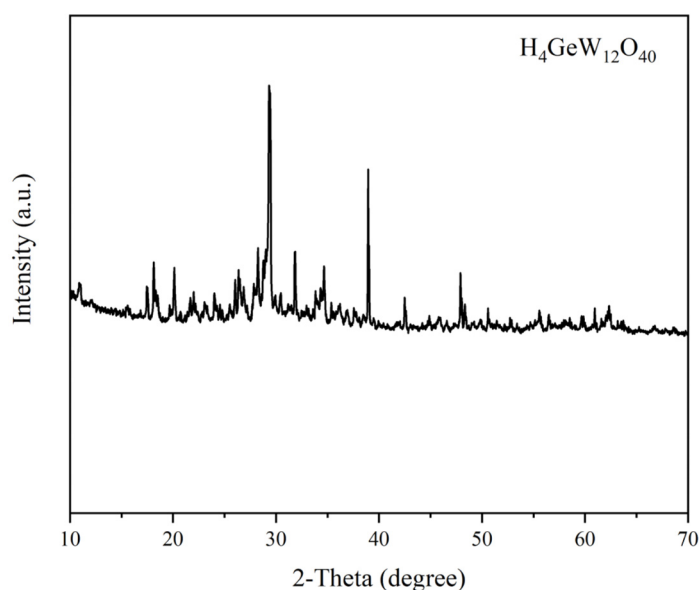


Figure 3. XRD patterns of prepared $\text{H}_4\text{GeW}_{12}\text{O}_{40}$.

The XPS spectra of $\text{H}_4\text{GeW}_{12}\text{O}_{40}$ are shown in Figure 4, and the high-resolution spectra of W 4f and C 1s were fitted. The W 4f high-resolution spectra were fitted with three typical peaks at 35.9 eV, 38.2 eV, and 41.7 eV, corresponding to W 4f_{7/2}, W 4f_{5/2}, and W 5p_{3/2}, respectively. Two single peaks exist in the C 1s high-resolution spectra, corresponding to C=C (284.6 eV), C-N, and C-C (285.8 eV). The measured results are essentially the same as the peak positions of the XPS spectra of $[\text{GeW}_{12}\text{O}_{40}]^{4-}$ anion in other literature [26], further suggesting that $\text{H}_4\text{GeW}_{12}\text{O}_{40}$ has a Keggin-type structure.

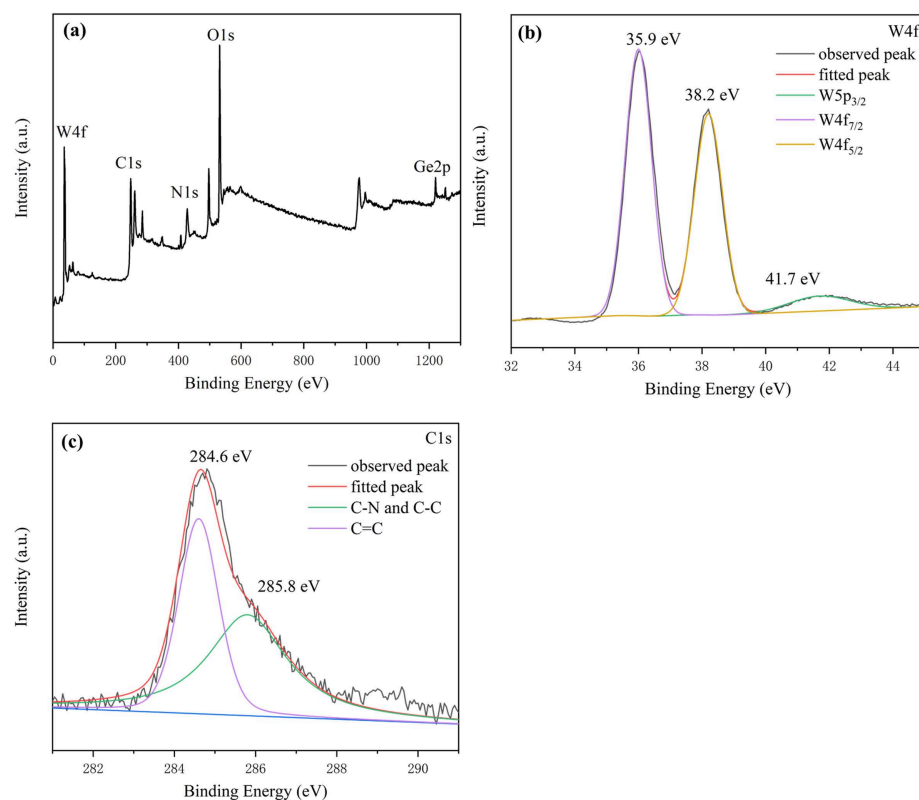


Figure 4. XPS spectra of $\text{H}_4\text{GeW}_{12}\text{O}_{40}$ ((a) survey spectrum; (b) W; (c) C.).

The morphology of the synthesized material was studied using SEM images (Figure 5a,b). Irregularly shaped structures can be found on the $H_4GeW_{12}O_{40}$ compound, and the size of the structures varies between 50 and 300 nm. The surface was found to contain a large number of small coarse particles at high magnification, which is also consistent with the surface morphological features described in the literature [27]. To further analyze the surface morphology, TEM images of c are shown in Figure 5c,d. Similar to the SEM results, Figure 5c shows the overall morphology of the catalyst similar to the SEM results. In Figure 5d, the morphology of the surface particles can be observed at higher magnification. Further BET tests were performed on the synthesized catalysts, and the surface area, pore volume, and pore size of $H_4GeW_{12}O_{40}$ are shown in Table 1.

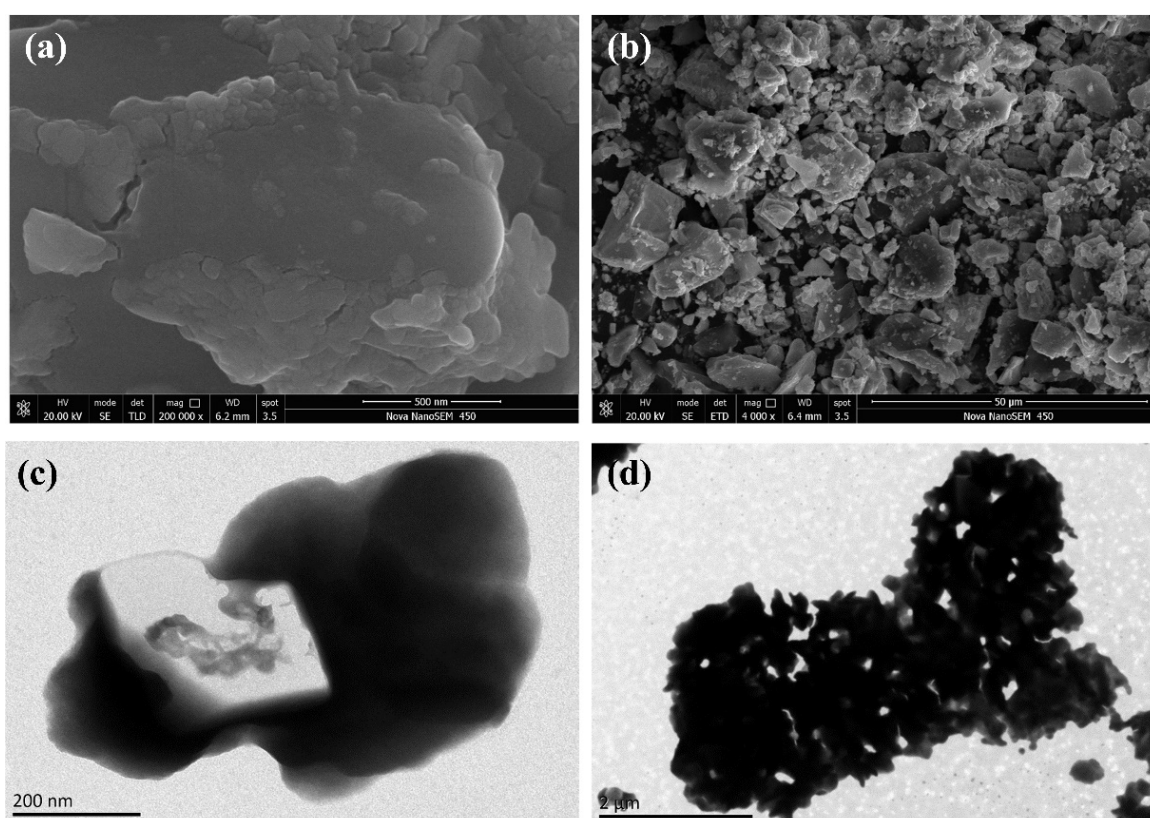


Figure 5. SEM images of $H_4GeW_{12}O_{40}$ (a,b) and the TEM images of $H_4GeW_{12}O_{40}$ (c,d).

Table 1. BET measurements of the as-synthesized Catalyst.

Catalyst	Surface Area [m^2/g]	Surface Area BJH_{Ads} [m^2/g]	Surface Area BJH_{Des} [m^2/g]	Pore Size BJH_{Ads} [nm]
$H_4GeW_{12}O_{40}$ Catalyst	2.21	2.57	2.09	4.9
$H_4GeW_{12}O_{40}$	Pore size BJH_{Des} [nm] 6.5	Pore volume BJH_{Ads} [cm^3/g] 0.032	Pore volume BJH_{Des} [cm^3/g] 0.031	

3.2. Catalytic Performance Evaluation

The catalytic activity of the Keggin-type HPAs on the oxidation removal of DBT was evaluated according to the experiments carried out at 35 °C for 60 min accompanied with ultrasound irradiation, using the above-mentioned experiment system with an initial sulfur concentration of 500 ppm, ozone dosage of 0.1 g/h, and a catalyst amount of 2.5 wt.% of *n*-octane. The results are shown in Table 1.

It can be observed from Table 2 that Keggin-type HPAs were effective in catalyzing ozone oxidation of DBT in simulated diesel. $H_3PMo_{12}O_{40}$ exhibited the best catalytic performance with a desulfurization efficiency of 93.3%, and the other W-containing HPAs

were inferior to it. The catalytic performance of the HPAs with Mo as polyatom was superior to those with W as polyatom. This result may be related to the oxidative ability of HPAs in that the oxidation capacity of Mo-containing heteropolyanions is higher than that of W-containing heteropolyanions [28,29].

Table 2. Catalytic effects of HPAs on the oxidation of DBT.

Catalyst	Efficiency (%)
H ₃ PW ₁₂ O ₄₀	89.3
H ₃ PMo ₁₂ O ₄₀	93.3
H ₄ SiW ₁₂ O ₄₀	85.7
H ₄ GeW ₁₂ O ₄₀	86.4
none	73.9

Among the catalyst HPAs with W as polyatom, the catalytic activity of H₃PW₁₂O₄₀ was the highest, reaching 89.3% of removal efficiency in 60 min. The removal of DBT catalyzed by H₄GeW₁₂O₄₀ and SiW₁₂O₄₀^{4−} was 86.4% and 85.7%, respectively. The catalytic activities of these catalysts increased in the order of H₄SiW₁₂O₄₀ < H₄GeW₁₂O₄₀ < H₃PW₁₂O₄₀, which agreed fairly well with the order of the oxidation potential of the polyanions, SiW₁₂O₄₀^{4−} < GeW₁₂O₄₀^{4−} < PW₁₂O₄₀ [3–7,10,11,19–23]. These results suggested that oxidative desulfurization was mainly affected by the oxidizing ability of HPAs.

Based on the results, it can be concluded that oxidizing ability of HPAs played a significant role in the ultrasound-assisted catalytic ozone oxidation process for desulfurization, and H₃PMo₁₂O₄₀ (HPMo) was chosen for additional experiments on the effects of several operational factors.

3.3. Influence of Reaction Conditions

3.3.1. Effect of Temperature

Temperature has a significant effect on DBT removal. From the results shown in Figure 6, it was evident that desulfurization efficiency decreased with the increase in temperature. At lower temperatures, such as at 0 °C, the desulfurization efficiency was 98.1% for a 60 min reaction, while with the temperature increased to 65 °C, the desulfurization efficiency decreased to 90.7%. The increase in temperature can influence the catalytic ozonation process in two ways: (1) the concentration of ozone in solution is reduced; (2) the diffusion rate of the reacting substances is enhanced. The efficiency decrease in DBT removal from 0 to 65 °C may demonstrate that (1) is predominant. Therefore, 0 °C can be recommended as the ideal temperature in this paper.

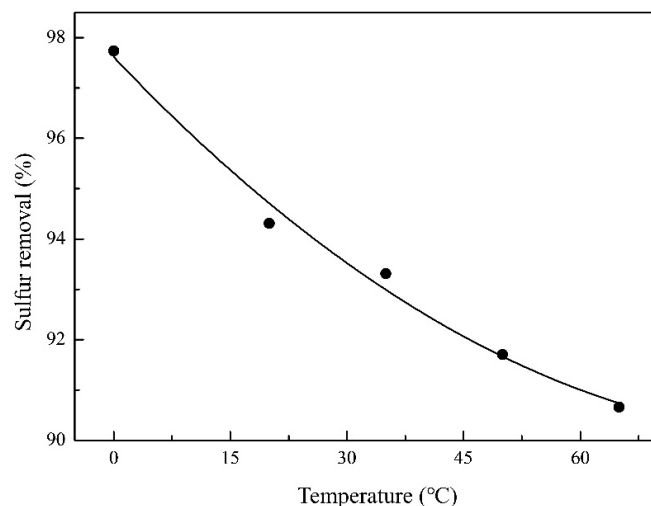


Figure 6. The effect of temperature on DBT removal. Experimental conditions: initial sulfur concentration, 500 ppm; catalyst dosage, 2.5 wt.% of *n*-octane; ozone dosage, 0.1 g/h; reaction time, 60 min.

3.3.2. Effect of Catalyst Dosage

Catalyst dosage also plays an important role in the oxidation of DBT. The results are presented in Figure 7. Under otherwise identical conditions, without catalyst, 71.5% of the DBT was removed from the *n*-octane phase in 60 min by the joint action of extraction and direct ozonation with ultrasonic irradiation. The efficiencies of DBT removal in the presence of HPMo increased remarkably from 88.4% to 98.1% with increasing weight percent of HPMo over the whole solution from 1.0 wt.% to 2.5 wt.%, and then leveled off from 2.5 wt.% to 3.0 wt.%. From the results, a suitable catalyst amount can be identified as 2.5 wt.% of the *n*-octane.

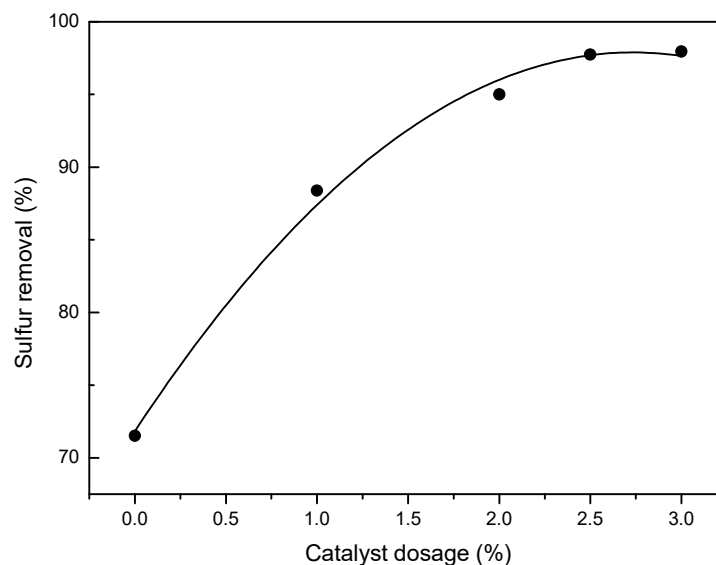


Figure 7. The effect of catalyst dosage on DBT removal. Experimental conditions: initial sulfur concentration, 500 ppm; temperature, 0 °C; ozone dosage, 0.1 g/h; reaction time, 60 min.

3.3.3. Effect of Initial Sulfur Concentration

Another significant factor for sulfur removal is the initial sulfur concentration, which was investigated using different concentrations (100, 300, 500, and 800 ppm). The results are shown in Figure 8. An increase in the initial sulfur concentration led to a remarkable decrease in the removal of DBT. When the initial sulfur concentration was 100 ppm, the conversion of DBT was up to 100% in 60 min, then as initial sulfur concentration increased to 300 ppm, 500 ppm, and further to 800 ppm, the desulfurization efficiency was found to decrease from 99.6% to 98.1%, and further to 85.9%, corresponding to 1.2 ppm, 10.0 ppm, and 112.8 ppm, respectively. This phenomenon indicated that DBT removal depends on its initial concentration, which may be caused by the decrease in catalytic active sites. As the initial concentration of DBT increased, more DBT molecules were absorbed into the catalyst. Thus, an increase in the amount of substrates accommodating the catalyst inhibits the action of the catalyst with O₃. Therefore, the desulfurization efficiency decreased.

3.3.4. Effect of Ultrasonic Irradiation

Ultrasonic irradiation can significantly enhance the reaction efficiency in chemical synthesis [30], since cavitation can be produced when mechanical vibrations are transmitted into the liquid as ultrasonic waves. In order to evaluate the effect of ultrasonic waves on the removal of DBT, a procedure applying the same previously optimized conditions was conducted, with a temperature of 0 °C, catalyst dosage of 2.5 wt.% of *n*-octane, and initial sulfur concentration of 500 ppm. However, mechanical stirring was employed instead of ultrasonic irradiation. The results are shown in Figure 9.

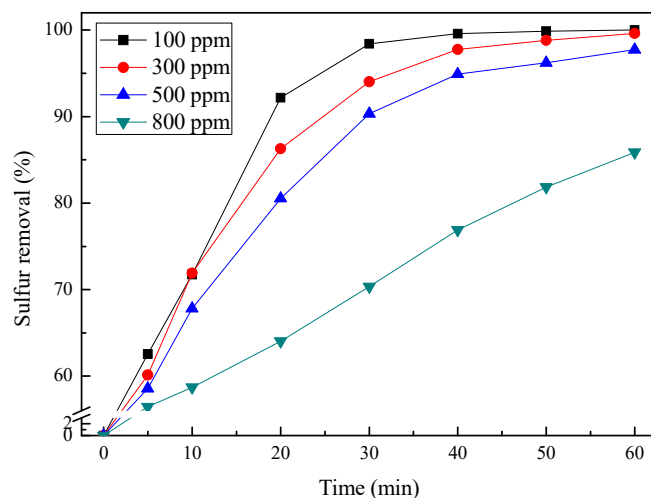


Figure 8. The effect of initial sulfur concentration on DBT removal. Experimental conditions: catalyst dosage, 2.5 wt.% of *n*-octane; temperature, 0 °C; ozone dosage, 0.1 g/h.

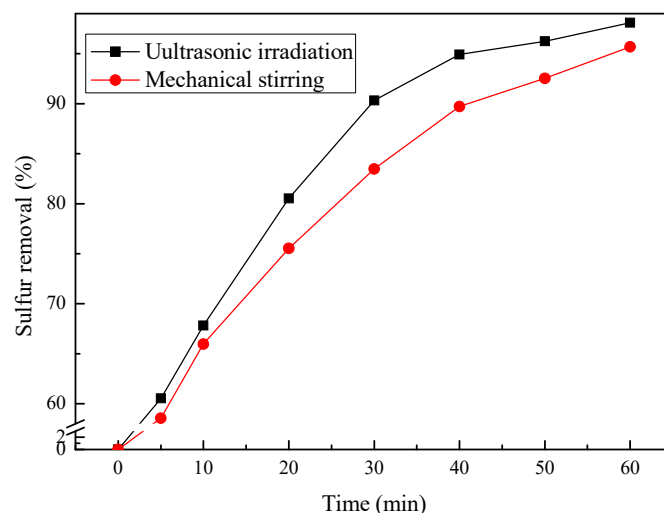


Figure 9. The effect of ultrasound on DBT removal. Experimental conditions: temperature, 0 °C; initial sulfur concentration, 500 ppm; catalyst dosage, 2.5 wt.% of *n*-octane; ozone dosage, 0.1 g/h; reaction time, 60 min.

The removal of DBT in catalytic ozonation with mechanical stirring was 94.5% for 60 min reaction. When ultrasonic irradiation was applied in catalytic ozonation, the removal of DBT increased to 98.1%. The efficiency of DBT removal with ultrasonic irradiation at different intervals evaluated were all higher than those with mechanical stirring. These results indicated that ultrasound enhances the mass transfer of ozone from the gas phase to the reaction solution and accelerates the whole desulfurization process. In this way, a better desulfurization effect is achieved.

3.3.5. Effect of Sulfide Species

To investigate the removal effect of HPMo on different sulfides, simulated diesel fuel with 500 ppm sulfur content of DBT, 4,6-DMDBT, and BT were configured to investigate the selectivity of the ODS system for different sulfides. As shown in Figure 10, the removal efficiencies of the sulfur compounds in the HPMo catalyst system were DBT > 4,6-DMDBT > BT. The reactivity of the thiophene sulfides was positively correlated with the electron cloud density of the sulfur atoms, which were 5.758, 5.760, and 5.739 for DBT, 4,6-DMDBT, and BT, respectively [31]. The low electron cloud density of the sulfur atoms of BT made it the most difficult of the three sulfides to remove, followed by 4,6-DMDBT, which was more

difficult to remove than DBT, probably due to the greater steric effects of 4,6-DMDBT on the molecular methyl group.

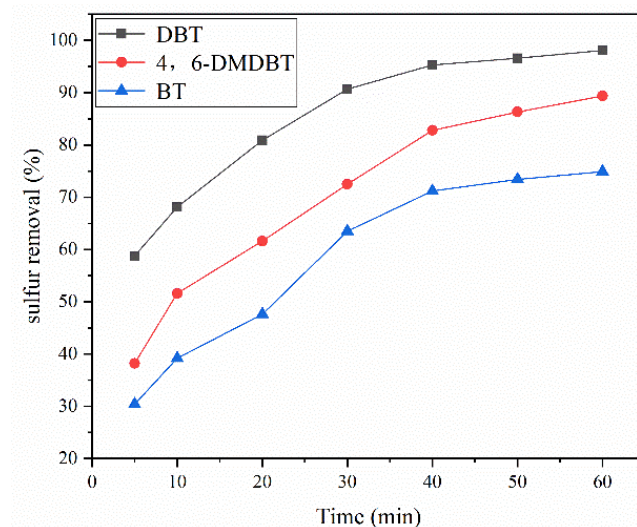


Figure 10. HPMo removal efficiency for different sulfides. Experimental conditions: temperature, 0 °C; initial sulfur concentration, 500 ppm; catalyst dosage, 2.5 wt.% of *n*-octane; ozone dosage, 0.1 g/h; reaction time, 60 min.

3.3.6. Catalyst Reuse

The catalytic effect of the used catalyst was explored and the recovering process was performed according to the method reported by Zhang et al. [32]. After completion of the reaction, the reaction mixture was kept still for 20 min. Then, the acetonitrile phase including the catalyst was separated and distilled to recover acetonitrile by cooling at the top of the distillation column. Water was added to the residue in the evaporator, and then, adding diethyl ether to the above mixture, HPMo was extracted into the diethyl ether phase. HPMo was recovered by further evaporation of diethyl ether. Evaluated through five recovery-reusing runs, the recovered HPMo catalyst was found to demonstrate excellent catalytic performance (Figure 11). The reused catalysts achieved 97%, 96.3%, 96.1%, 95.8%, and 94.9% DBT conversions in the first, second, third, fourth and fifth ODS cycles, respectively.

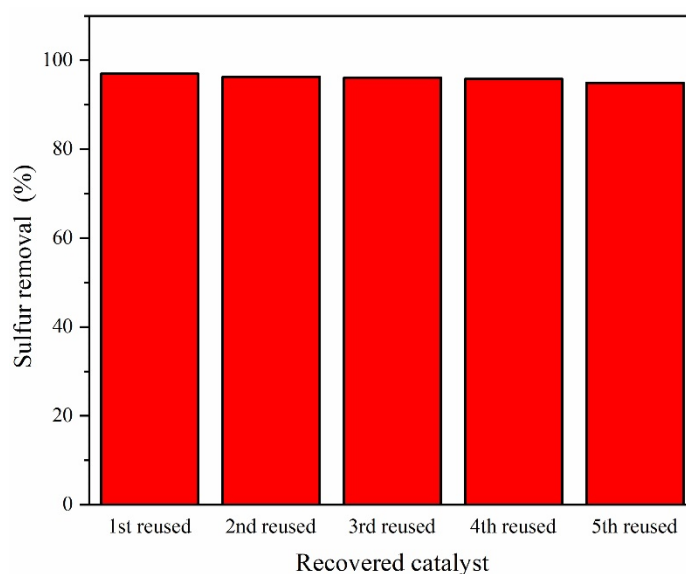


Figure 11. The ODS performance of the reused catalyst.

4. Conclusions

Ultrasound-assisted catalytic ozone oxidation process exhibited high efficiency for the removal of DBT from simulated diesel. The catalytic performance of Keggin-type HPAs was mainly related to the oxidizing ability of HPAs and followed the order of $\text{H}_3\text{PMo}_{12}\text{O}_{40} > \text{H}_3\text{PW}_{12}\text{O}_{40} > \text{H}_4\text{SiW}_{12}\text{O}_{40} > \text{H}_4\text{GeW}_{12}\text{O}_{40}$ in the desulfurization process. Factors affecting the ODS process were investigated, including temperature, catalyst dosage, initial sulfur content, and ultrasound irradiation, whereby the favorable operating conditions were recommended as reaction temperature, 0 °C; catalyst dosage, 2.5 wt.% of *n*-octane; and ultrasound irradiation. DBT removal depended on its initial concentration, and increasing initial sulfur concentration led to a decrease in desulfurization efficiency. Furthermore, the used catalyst was recoverable and demonstrated excellent catalytic performance. As a whole, the ultrasound-assisted catalytic ozone oxidation process has a good application prospect to obtain ultra-low sulfur diesel.

Author Contributions: K.Z.: investigation, writing original draft, writing—review and editing. R.W. and I.V.K.: project administration, funding acquisition, writing—review and editing. All authors have read and agreed to the published version of the manuscript.

Funding: This research was funded by the National Natural Science Foundation of China (Nos. 20976097, 21076116, 21211120165, 21311120297), Petro China Scientific and Technical Innovation Project (2010D-5006-0405), and Natural Science Foundation of Shandong Province (ZR2018MEE048).

Institutional Review Board Statement: Not applicable.

Informed Consent Statement: Not applicable.

Data Availability Statement: Not applicable.

Acknowledgments: Special thanks to the School of Environment, Shandong University for its public research platform.

Conflicts of Interest: The authors declare no conflict of interest.

Sample Availability: Samples of the $\text{H}_3\text{PMo}_{12}\text{O}_{40}$ are available from the authors.

References

1. Lü, H.; Zhang, Y.; Jiang, Z.; Li, C. Aerobic oxidative desulfurization of benzothiophene, dibenzothiophene and 4,6-dimethyldibenzothiophene using an Anderson-type catalyst $[(\text{C}_{18}\text{H}_{37})_2\text{N}(\text{CH}_3)_2]_5[\text{IMo}_6\text{O}_{24}]$. *Green. Chem.* **2010**, *12*, 1954–1958. [[CrossRef](#)]
2. Jiang, C.; Wang, J.; Wang, S.; Guan, H.; Wang, X.; Huo, M. Oxidative desulfurization of dibenzothiophene with dioxygen and reverse micellar peroxotitanium under mild conditions. *Appl Catal. B Environ.* **2011**, *106*, 343–349. [[CrossRef](#)]
3. Wang, R.; Yu, F.; Zhang, G.; Zhao, H. Performance evaluation of the carbon nanotubes supported $\text{Cs}_{2.5}\text{H}_{0.5}\text{PW}_{12}\text{O}_{40}$ as efficient and recoverable catalyst for the oxidative removal of dibenzothiophene. *Catal. Today* **2010**, *150*, 37–41. [[CrossRef](#)]
4. Jiang, Z.; Lü, H.; Zhang, Y.; Li, C.J. Oxidative desulfurization of fuel oils. *Chin. J. Catal.* **2011**, *32*, 707–715. [[CrossRef](#)]
5. Oyama, S.T. Chemical and catalytic properties of ozone. *Catal. Rev.* **2000**, *42*, 279–322. [[CrossRef](#)]
6. He, Z.; Cai, Q.; Hong, F.; Jiang, Z.; Chen, J.; Song, S. Effective Enhancement of the Degradation of Oxalic Acid by Catalytic Ozonation with TiO_2 by Exposure of {001} Facets and Surface Fluorination. *Ind. Eng. Chem. Res.* **2012**, *51*, 5662–5668. [[CrossRef](#)]
7. Hasan, M.T.; Senger, B.J.; Ryan, C.; Culp, M.; Gonzalez-Rodriguez, R.; Coffey, J.L.; Naumov, A.V. Optical band gap alteration of graphene oxide via ozone treatment. *Sci. Rep.* **2017**, *7*, 6411. [[CrossRef](#)]
8. Gaudino, E.C.; Carnaroglio, D.; Boffa, L.; Cravotto, G.; Moreira, E.M.; Nunes, M.A.; Flores, E.M. Efficient $\text{H}_2\text{O}_2/\text{CH}_3\text{COOH}$ oxidative desulfurization/denitrification of liquid fuels in sonochemical flow-reactors. *Ultrason. Sonochem.* **2014**, *21*, 283–288. [[CrossRef](#)]
9. Carnaroglio, D.; Gaudino, E.C.; Mantegna, S.; Moreira, E.M.; Vicente de Castro, A.; Flores, E.M.; Cravotto, G. Ultrasound-assisted oxidative desulfurization/denitrification of liquid fuels with solid oxidants. *Energy Fuels* **2014**, *28*, 1854–1859. [[CrossRef](#)]
10. Enferadi-Kerenkan, T.; Do, O.; Kaliaguine, S. Heterogeneous catalysis by tungsten-based heteropoly compounds. *Catal. Sci. Technol.* **2018**, *8*, 2257–2284. [[CrossRef](#)]
11. Shatalov, A.; Pereira, H. Polyoxometalate catalyzed ozonation of chemical pulps in organic solvent media. *Chem. Eng. J.* **2009**, *155*, 380–387. [[CrossRef](#)]
12. Shatalov, A.; Pereira, H. Molybdo-vanado-phosphate heteropolyanion catalyzed pulp ozonation in acetone/water solution. Part 2. Catalyst re-oxidation. *Bioresour. Technol.* **2010**, *101*, 9330–9334. [[CrossRef](#)]

13. Craven, M.; Xiao, D.; Kunstmann-Olsen, C.; Kozhevnikova, E.F.; Blanc, F.; Steiner, A.; Kozhevnikov, I.V. Oxidative desulfurization of diesel fuel catalyzed by polyoxometalate immobilized on phosphazene-functionalized silica. *Appl. Catal. B* **2018**, *231*, 82–91. [[CrossRef](#)]
14. Rafiee, E.; Nobakht, N.J. Keggin type heteropoly acid, encapsulated in metal-organic framework: A heterogeneous and recyclable nanocatalyst for selective oxidation of sulfides and deep desulfurization of model fuels. *J. Mol. Catal. A Chem.* **2015**, *398*, 17–25. [[CrossRef](#)]
15. Shafiq, I.; Hussain, M.; Rashid, R.; Shafique, S.; Akhter, P.; Yang, W.; Park, Y.K. Development of hierarchically porous LaVO₄ for efficient visible-light-driven photocatalytic desulfurization of diesel. *Chem. Eng. J.* **2021**, *420*, 130529. [[CrossRef](#)]
16. Li, S.W.; Wang, W.; Zhao, J.S. Effective and reusable oxidative desulfurization of dibenzothiophene via magnetic amino-MIL-101 supported H₃PMo₆W₆O₄₀ components: Comparison influence on various types of MIL-101. *Energy Fuels* **2020**, *34*, 4837–4848. [[CrossRef](#)]
17. Li, S.W.; Zhang, H.Y.S.M.; Dong, J.S.; Zhao, R.X.; Li, J. Highly efficient preformed heteropolyacid catalysts for the deep oxidative desulfurization: MOF as a bridge role under nucleation theory. *Environ. Chem. Eng.* **2022**, *10*, 107298. [[CrossRef](#)]
18. Wang, R.; Zhao, Y.; Kozhevnikov, I.V.; Zhao, J. An ultrasound enhanced catalytic ozonation process for the ultra-deep desulfurization of diesel oil. *New J. Chem.* **2020**, *44*, 15467–15474. [[CrossRef](#)]
19. Micek-Ilnicka, A.J. The role of water in the catalysis on solid heteropolyacids. *J. Mol. Catal. A Chem.* **2009**, *308*, 1–14. [[CrossRef](#)]
20. Wang, Z.P.; Niu, J.Y.; Xu, L. Thermal properties study of Keggin structured heteropolyacids. *Chim. Sin.* **1995**, *53*, 757–764.
21. Wu, Q.; Song, Y.; Wang, E. Application of tungsten acid in butyl synthesis. *Chem. Reagent* **1993**, *15*, 4–5. (In Chinese)
22. Baronetti, G.; Briand, L.; Sedran, U.; Thomas, H. Heteropolyacid-based catalysis. Dawson acid for MTBE synthesis in gas phase. *Appl. Catal. A Gen.* **1998**, *172*, 265–272. [[CrossRef](#)]
23. Rocchiccioli-Deltcheff, C.; Fournier, M.; Franck, R.; Thouvenot, R. Vibrational investigations of polyoxometalates. 2. Evidence for anion-anion interactions in molybdenum (VI) and tungsten (VI) compounds related to the Keggin structure. *Inorg. Chem.* **1983**, *22*, 207–216. [[CrossRef](#)]
24. Hodjati, S.; Vaezzadeh, K.; Petit, C.; Pitchon, V.; Kiennemann, A. The mechanism of the selective NO_x sorption on H₃PW₁₂O₄₀·6H₂O (HPW). *Top. Catal.* **2001**, *16*, 151–155. [[CrossRef](#)]
25. Sun, Y.; Liu, S.X.; Liang, D.D.; Shao, K.Z.; Ren, Y.H.; Su, Z.M. Highly stable crystalline catalysts based on a microporous metal–organic framework and polyoxometalates. *J. Am. Chem. Soc.* **2009**, *131*, 1883–1888. [[CrossRef](#)]
26. Hu, Y.Y.; Xiao, L.N.; Wang, Y.; Zhao, D.C.; Wang, L.M.; Guo, H.Y.; Gui, X.B.; Xu, J.Q. New compounds based on polyoxometalates and transition metal complexes with a lower positive charge. *Polyhedron* **2013**, *56*, 152–159. [[CrossRef](#)]
27. Wu, Q.; Tao, S.; Lin, H.; Meng, G. Preparation and conductivity of solid high-proton conductor silica gels containing 12-tungstogermanic heteropoly acid. *Mater. Sci. Eng. B* **2000**, *68*, 161–165. [[CrossRef](#)]
28. Misono, M. Heterogeneous catalysis by heteropoly compounds of molybdenum and tungsten. *Catal. Rev.* **1987**, *29*, 269–321. [[CrossRef](#)]
29. Hanif, M.A.; Nisar, S.; Rashid, U. Supported solid and heteropoly acid catalysts for production of biodiesel. *Catal. Rev.* **2017**, *59*, 165–188. [[CrossRef](#)]
30. Mello, P.D.A.; Duarte, F.A.; Nunes, M.A.; Alencar, M.S.; Moreira, E.M.; Korn, M.; Dresslera, V.L.; Flores, É.M. Ultrasound-assisted oxidative process for sulfur removal from petroleum product feedstock. *Ultrason. Sonochem.* **2009**, *16*, 732–736. [[CrossRef](#)]
31. Otsuki, S.; Nonaka, T.; Takashima, N.; Qian, W.; Ishihara, A.; Imai, T.; Kabe, T. Oxidative desulfurization of light gas oil and vacuum gas oil by oxidation and solvent extraction. *Energy Fuels* **2000**, *14*, 1232–1239. [[CrossRef](#)]
32. Zhang, G.; Wang, R.; Yu, F.; Zhao, H. Clean fuel-oriented investigation of thiophene oxidation by hydrogen peroxide using polyoxometalate as catalyst. *Chem. Pap.* **2009**, *63*, 617–619. [[CrossRef](#)]